International Journal of Pharmaceutics 468 (2014) 26–38

Contents lists available at ScienceDirect

International Journal of Pharmaceutics

journal homepage: www.elsevier.com/locate/ijpharm

Pharmaceutical nanotechnology

Increased tumor targeted delivery using a multistage liposome system functionalized with RGD, TAT and cleavable PEG

Ling Mei [1], Ling Fu [1], Kairong Shi, Qianyu Zhang, Yayuan Liu, Jie Tang, Huile Gao, Zhirong Zhang, Qin He *

Key Laboratory of Drug Targeting and Drug Delivery Systems, West China School of Pharmacy, Sichuan University. No. 17, Block 3, Southern Renmin Road, Chengdu 610041, PR China

ARTICLE INFO

Article history:
Received 3 April 2014
Received in revised form 3 April 2014
Accepted 3 April 2014
Available online 5 April 2014

Keywords:
Tumor targeting
Multistage liposome
Cleavable PEG
Synergistic effect

ABSTRACT

Though PEGylation has been widely used to enhance the accumulation of liposomes in tumor tissues through enhanced permeability and retention (EPR) effects, it still inhibits cellular uptake and affects intracellular trafficking of carriers. Active targeting molecules displayed better cell selectivity but were shadowed by the poor tumor penetration effect. Cell penetrating peptides could increase the uptake of the carriers but were limited by their non-specificity. Dual-ligand system may possess a synergistic effect and create a more ideal drug delivery effect. Based on the above factors, we designed a multistage liposome system co-modified with RGD, TAT and cleavable PEG, which combined the advantages of PEG, specific ligand and penetrating peptide. The cleavable PEG could increase the stability and circulation time of liposomes during circulation. After the passive extravasation to tumor tissues, the previously hidden dual ligands on the liposomes were exposed in a controlled manner at the tumor site through exogenous administration of a safe reducing agent L-cysteine. The RGD specifically recognized the integrins overexpressed on various malignant tumors and mediated efficient internalization in the synergistic effect of the RGD and TAT. *In vitro* cellular uptake and 3D tumor spheroids penetration studies demonstrated that the system could not only be selectively and efficiently taken up by cells overexpress ingintegrins but also penetrate the tumor cells to reach the depths of the avascular tumor spheroids. *In vivo* imaging and fluorescent images of tumor section further demonstrated that this system achieved profoundly improved distribution within tumor tissues, and the RGD and TAT ligands on C-R/T liposomes produced a strong synergistic effect that promoted the uptake of liposomes into cells after the systemic administration of L-cysteine. The results of this study demonstrated a tremendous potential of this multistage liposomes for efficient delivery to tumor tissue and selective internalization into tumor cells.

1. Introduction

In recent years, various drug delivery systems (DDS) have been developed that can provide targeted delivery of anticancer drugs to tumor tissue, but the DDS may be recognized and quickly cleared by the reticuloendothelial system (RES) (Sapra et al., 2005), this effect hindered the further transfer of DDS *in vivo*. PEGylation of nanocarriers can avoid carriers binding with plasma proteins and removal by RES, thus prolonging the circulation time of carriers (Klibanov et al., 1990) and making nanocarriers accumulate in tumor tissue via the enhanced permeability and retention (EPR) effect (Maeda, 2012). Moreover, previous studies have found that the passive targeting capability of EPR effect also has great significance in the active targeting carriers. Carries may accumulate in tumor mainly via EPR effect, then the carries were efficiently internalized by the function of active ligands (Hatakeyama et al., 2007a,b). However, PEGylation seriously hindered the interactions between the DDS and cells after arriving at tumor tissues (Gullotti and Yeo, 2009). Using cleavable PEG instead of traditional PEG to modify the DDS (Wu et al., 2012; Koren et al., 2012) can provide long circulating properties and avoid the impact of PEG on the binding of carriers with targeted cells. Several ways have been reported for the cleavage of PEG after arrival at tumor tissue, including the conjugation of PEG onto the surface of liposomes via pH sensitive (Kale and Torchilin., 2007; Sawant et al., 2006), MMP sensitive (Terada et al.,2006) esterase sensitive (Xu et al., 2008) or

* Corresponding author. Tel.: +86 28 85502532; fax: +86 28 85502532.
E-mail addresses: qinhe@scu.edu.cn, qinhe317@126.com (Q. He).
[1] These authors contributed equally to this work.

http://dx.doi.org/10.1016/j.ijpharm.2014.04.008
0378-5173/

reductive potential sensitive (McNeeley et al., 2009) chemical bonds; among these approaches, reductive potential sensitive chemical bonds such as disulfide are easy to construct and can be cleaved precisely by a safe cleaving agent L-cysteine (L-Cys).

TAT peptide (AYGRKKRRQRRR) is a well-known CPP, which is the basic region of the trans-activating transcriptional activator protein from HIV-1 (Torchilin, 2008), and it is able to transport different molecules and even 200 nm nanocarriers across biological barriers to be taken up by various cell lines (Duchardt et al., 2007; Pappalardo et al., 2009). In our previous study, TAT could be masked by the longer cleavable PEG spacer and the penetrating ability of the CPP was effectively shielded during circulation (Kuai et al., 2010, 2011). Upon reaching sufficient accumulation in the tumor tissue, protective PEG attached to the surface of the DDS via the disulfide bond was detached under the action of reducing agent L-cysteine and the previous hidden TAT was exposed, allowing for the subsequent delivery of the carrier and its cargos inside cells. However, TAT does not have cell-type specificity and mainly relies on the electrostatic interaction of its positively charged amino acids with negatively charged cell-surface glycoproteins (Marcucci and Lefoulon, 2004), and this drawback greatly limited its targeted application.

Compared to the CPPs, active targeting molecules such as monoclonal antibody, polypeptide and nucleic acid fragments can make the DDS identify specific cells with strong cell selectivity (Burks et al., 2010; Matteo et al., 2006). Among all the cancer-specific ligands, cRGDfK peptide, cyclic (arginine–glycine–aspartic acid–phenylalaninelysine), has been widely employed as a targeting moiety for various anticancer drugs and nanocarriers (Oba et al., 2007; Gao et al., 2014a,b,c). RGD is an adhesion motif of extracellular matrix proteins for the various types of integrins, especially $\alpha_v\beta_3$ and $\alpha_v\beta_5$, which are overexpressed on the angiogenic endothelium in diseased tissues and various malignant tumors. However, the long circulating effect of PEG can be compromised by the presence of receptor-targeting ligands on the nanocarrier surface, especially at higher ligand densities (Khalil et al., 2006; Xiong et al., 2005). The targeting ligands on the nanocarrier surface can bind to plasma proteins (Kaasgaard et al., 2001), and the presence of targeting ligands may evoke immune responses, prohibiting repeated dosing of the formulation (Harding et al., 1997). Moreover, receptor-mediated endocytosis is a saturated pathway, which limits the cellular uptake of DDS, and the internalization of DDS modified with active targeting molecules is relatively weak (McNeeley et al., 2007; Yang et al., 2012).

Some recent studies have suggested a strategy combining the advantages of specific ligands with CPPs may possess a more ideal drug delivery effect (Xiong et al., 2010; Takara et al., 2012; Gao et al., 2013a,b), which showed better cell selectivity and efficient cargo delivery. Taking the "shielding" effect of cleavable PEG into consideration, we established a multistage liposome system modified with RGD, TAT and cleavable PEG, and the liposome can accumulate in the tumor tissue and efficiently be taken up into tumor cells. The multistage liposome system has a three-tier cascade structure (Fig. 1). The outermost shielding layer was constituted by the longest cleavable PEG chain (PEG_{5000}), which could mask the dual ligands, increase the stability of liposomes and possess prolonged circulation time. The middle layer was cell recognizing and binding layer, which was constituted by specific ligand RGD connected with comparatively shorter PEG chain (PEG_{3500}). The inner layer was cell penetrating layer, which was constituted by TAT connected to the end of the shortest PEG spacer (PEG_{1000}). After the passive extravasation to tumor tissues, the previous hidden dual ligands were exposed through exogenous administration of a safe reducing agent L-cysteine at the tumor site. The RGD specifically recognized the integrins and bound to the cell surface, pulling the TAT closer to the cell surface which mediated more efficient internalization in the synergistic effect of the RGD and TAT.

2. Materials and methods

2.1. Materials

cRGDfK-cysteine peptide (cycle RGDfK-cys) and TAT-cysteine peptide (Cys-AYGRKKRRQRRR) were synthesized according to the standard solid phase peptide synthesis by Chinapeptides Co., Ltd. (Shanghai, China) and Chengdu KaiJie Bio-pharmaceutical Co., Ltd. (Chengdu, China). SPC was purchased from Taiwei Chemical Company (Shanghai, China). Cholesterol was purchased from Kelong Chemical Company (Chengdu, China). 1,2-Distearoyl-sn-glycero-3-phosphoethanolamine (DSPE), 1,2-distearoyl-sn-glycero-3-phosphoethanolamine-poly(ethylene glycol) 2000 (DSPE-PEG_{2000}) and 1,2-dioleoyl-sn-glycero-3-phosphoethanolamine-*N*-(carboxyfluorescein) (CFPE) were purchased from Avanti Polar Lipids (Alabaster, AL, USA). NHS-PEG_{1000}-Mal, NHS-PEG_{3500}-Mal, PEG_{5000}-SH and PEG_{5000}-NHS were obtained from Jenkem Technology (Beijing, China). *N*-Succinimidyl-3-(2-pyridyldithio) propionate (SPDP) was purchased from Sigma (China, mainland). 1,1′-Dioctadecyl-3,3,3′,3′-tetramethylindotricarbocyanine iodide (DIR) and 1,1′-dioctadecyl-3,3,3′,3′-tetramethylindodicarbocyanine 4-chlorobenzenesulfonate salt (DID) were purchased from Biotium. All of other reagents and chemicals were analytical grade and were used without further purification.

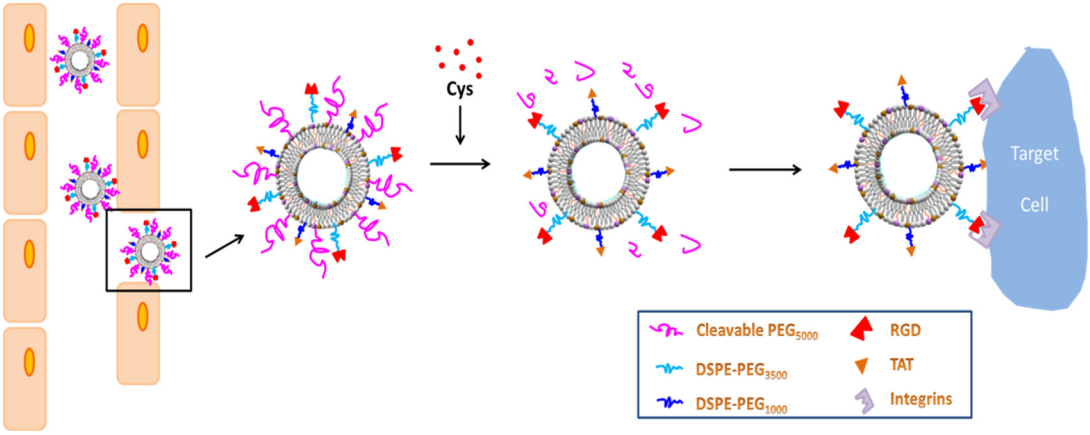

Fig. 1. Schematic illustrations of the multistage liposomes modified with RGD, TAT and cleavable PEG(C-R/T).

2.2. Synthesis of DSPE-PEG$_{1000}$-TAT and DSPE-PEG$_{3500}$-RGD

NHS-PEG-Mal (NHS-PEG$_{1000}$-Mal/NHS-PEG$_{3500}$-Mal) was reacted with an approximately 1.5-fold molar excess of DSPE in dry chloroform at room temperature under argon with a 3-fold molar excess of triethylamine for about 5 h. The reaction was traced by TLC till the NHS-PEG-Mal was completely consumed. The excess DSPE was removed by adding an appropriate amount of acetonitrile to precipitate it. After that, the supernatant was collected and evaporated. The obtained DSPE-PEG$_{1000}$-Mal was used for the next reaction.

The obtained DSPE-PEG$_{1000}$-Mal was reacted with an approximately 1.5-fold molar excess of Cys-TAT in the mixture of $CHCl_3$/MeOH (V:V = 2:1) at room temperature with stirring for about 30 h, and the reaction was traced by TLC till the DSPE-PEG$_{1000}$-Mal was completely consumed, and the slight excess of Cys-TAT was removed by adding a small volume of $CHCl_3$. The insoluble material was filtered, and the supernatant was evaporated. The synthesis was confirmed by mass spectroscopy and thin-layer chromatography.

A DSPE-PEG$_{3500}$-Mal lipid film was formed by evaporation of the solvents (chloroform) from the lipid solution. The DSPE-PEG$_{3500}$-Mal film was hydrated with PBS buffer (pH 7.4), followed by a 2 min bath-type sonication to form micelle. Then the DSPE-PEG$_{3500}$-Mal micellewas reacted with an approximately 1.5-fold molar excess of cRGDfK-Cys in PBS buffer (pH 7.4) at 4 °C for 48 h, and the reaction was traced by TLC till the DSPE-PEG$_{3500}$-Mal was completely consumed. The excess cRGDfK-Cys was separated on a Sephadex-G50 column using PBS buffer (pH 7.4). The fraction containing product was lyophilized and then extracted twice with chloroform to remove inorganic salts, the chemical structure of the DSPE-PEG$_{3500}$-RGD was confirmed by mass spectroscopy.

2.3. Synthesis of DSPE-S-S-PEG$_{5000}$ and DSPE-PEG$_{5000}$-OMe

DSPE-S-S-PEG$_{5000}$ was synthesized as described previously with some modification. Briefly, an approximately 1.25-fold molar excess of DSPE was reacted with SPDP by stirring for 5 h in dry chloroform at 55 °C with a 3-fold molar excess of triethylamine, and the reaction was traced by TLC till the SPDP was completely consumed, and the PEG$_{5000}$-SH was added. The mixture was allowed to react in dark under argon at 45 °C for about 48 h. The excess DSPE was separated from the product by adding an appropriate amount of acetonitrile to precipitate it. After that, the supernatant was collected and evaporated. The residue was recrystallized twice from diethyl ether and then purified on a silica column, using $CHCl_3$/MeOH mixtures of different volume ratios (which were 50:0.5, 50:1, 50:1.5, 50:2 and 50:15, respectively). The chemical structure was verified by mass spectroscopy.

NHS-PEG$_{5000}$-OMe was reacted with an approximately 1.5-fold molar excess of DSPE in dry chloroform at 55 °C under argon with a 3-fold molar excess of triethylamine for about 2 h, and the reaction was traced by TLC till the NHS-PEG$_{5000}$-OMe was completely consumed. The excess DSPE was separated from the product by adding an appropriate amount of acetonitrile to precipitate it. After that, the supernatant was collected and evaporated, and the residue was recrystallized twice from diethyl ether. The chemical structure was verified by mass spectroscopy.

2.4. Preparation and characterization of liposomes

Liposomes were prepared by the lipid hydration method (Schiffelers et al., 2003). The liposomes used in this study included the conventional long-circulating PEG liposome (PEG), the non-cleavable PEG and RGD/TAT co-modified liposome (N-R, N-T), the cleavable PEG and RGD/TAT co-modified liposome (C-R, C-T), the non-cleavable/cleavable PEG, RGD and TAT co-modified liposome (N-R/T, C-R/T). Their basic composition was SPC/CHO = 2:1, and various lipid materials (see Table 1) were added to the lipid solution. A lipid film was formed by evaporation of the solvents (chloroform: ethanol = 2:1) from the lipid solution, the obtained thin film was kept in vacuum for over 6 h to completely remove the residual organic solvent. The lipid film was hydrated with PBS buffer (pH 7.4), followed by a 1 h (37 °C) incubation and a 2 min bath-type sonication. Then it was sonicated with aprobe-type sonicator at 80 W power for 45 s. During film formation, fluorescently labeled materials (12 μg/mL CFPE, 20 μg/mL DIR or 20 μg/mL DID) was incorporated to label the lipid composition.

The mean sizes and zeta potentials of the prepared liposomes were determined using a Malvern Zetasizer Nano ZS 90 instrument (Malvern instruments Ltd., UK).

2.5. Stability of liposomes in the presence of fetal bovine serum

A total of 100 μL of different formulations of liposomes were diluted with medium containing 50% fetal bovine serum (FBS) or PBS buffer (pH 7.4) to 1 ml and incubated at 37 °C for 24 h (Hansen et al., 2012). The variance of particle size was measured by dynamic light scattering.

2.6. In vitro *cellular uptake*

2.6.1. Cell culture

The human hepatoma cells (HepG2) were cultured in RPMI-1640 medium (GIBCO), human cervical carcinoma cells (Hela) were cultured in DMEM medium (GIBCO), respectively, which contained 10% FBS, streptomycin (100 μg/mL) and penicillin (100 U/mL). The cells were maintained under an atmosphere of 5% CO_2 at 37 °C.

2.6.2. Quantitative analysis of cellular uptake by flow cytometry(FACS)

HepG2 and Hela cells were seeded respectively onto six-well plate at a density of 5×10^5 per well and incubated overnight at 37 °C in an atmosphere of 5% CO_2 and 95% humidity before further experiments. After 24 h, it was replaced with fresh serum-free medium, and then the prepared CFPE-labeled liposomes were

Table 1
Sizes and zeta potentials of different formulations of liposomes[a].

Sample ID	Composition	Size (nm)	PDI	Zeta potential (mV)
PEG	0.5%DSPE-PEG$_{1000}$ + 1%DSPE-PEG$_{3500}$	99.05 ± 0.92	0.19 ± 0.00	−5.95 ± 1.26
RGD	0.5%DSPE-PEG$_{1000}$ + 1%DSPE-PEG$_{3500}$-RGD	107.53 ± 2.68	0.23 ± 0.02	−3.54 ± 1.13
TAT	0.5%DSPE-PEG$_{1000}$-TAT + 1%DSPE-PEG$_{3500}$	101.37 ± 2.99	0.20 ± 0.01	−1.42 ± 0.76
R/T	0.5%DSPE-PEG$_{1000}$ + 1%DSPE-PEG$_{3500}$-RGD	113.23 ± 2.61	0.25 ± 0.02	−0.50 ± 1.55
C-RGD	0.5%DSPE-PEG$_{1000}$ + 1%DSPE-PEG$_{3500}$-RGD + 8%DSPE-S-S-PEG$_{5000}$	86.31 ± 0.42	0.24 ± 0.01	−3.23 ± 0.65
C-TAT	0.5%DSPE-PEG$_{1000}$-TAT + 1%DSPE-PEG$_{3500}$ + 8%DSPE-S-S-PEG$_{5000}$	84.34 ± 6.44	0.19 ± 0.03	−1.57 ± 1.26
C-R/T	0.5%DSPE-PEG$_{1000}$-TAT + 1%DSPE-PEG$_{3500}$-RGD + 8%DSPE-S-S-PEG$_{5000}$	89.41 ± 0.80	0.22 ± 0.04	−1.18 ± 0.92
N-R/T	0.5%DSPE-PEG$_{1000}$-TAT + 1%DSPE-PEG$_{3500}$-RGD + 8%DSPE-PEG$_{5000}$-OMe	89.73 ± 8.93	0.18 ± 0.01	−0.90 ± 0.43

[a] Data are expressed as the mean ± SD, $n = 3$.

added to the cells. The final lipid concentration was 0.2 mg/mL. After incubation for 4 h, the medium was discarded and the cells were washed three times with cold PBS. Cells were harvested and washed with cold PBS, centrifuged at 4000 rpm and re-suspended for three times (Li et al., 2012). The cellular uptake efficiency was determined by FACS.

2.6.3. Qualitative analysis of cellular uptake by confocal laser scanning microscopy (CLSM)

HepG2 and Hela cells were seeded respectively on coverslips at a density of 2.5×10^5 per well in a six-well plate. After 24 h cultivation, cells were incubated with CFPE-labeled liposomes for4 h at 37 °C. Then the cells were washed three times with cold PBS (pH 7.4) and fixed with 4% paraformaldehyde. 0.5 mL of DAPI was added to stain the nuclei for an additional 5 min. Coverslipswere mounted cell-side down with slides and viewed using a Leica TCS SP5 AOBS confocal microscopy system (Leica, Germany).

2.7. Identification of cellular uptake pathways

2.7.1. The cellular uptake of modified liposomes in HepG2 in the presence of various endocytosis inhibitors

Cellular uptake mechanism of CFPE-labeled liposomes was assessed by using inhibitors for specific endocytosis pathways. Endocytosis inhibitors NaN_3 (10 mM), poly-lysine (800 μg/mL), colchicine (4 μg/mL), chlorpromazine (20 μg/mL) and filipin (5 μg/mL) were added to HepG2 cells for 30 min before, the incubation with liposomes for another 4 h at 37 °C. Influence of the temperature on the cellular uptake was evaluated by incubating HepG2 cells with liposomes for 4 h at 4 °C (Hansen et al., 2012). Following washes with PBS as described above, cellular uptake was evaluated by flow cytometry.

2.7.2. The binding and internalization of C-R/T liposomes in HepG2 in the presence of free RGD

HepG2 cells were seeded on coverslips at a density of 2.5×10^5 per well in a six-well plate. After 24 h cultivation, a 50-fold molar excess of free RGD was added into the medium for 1 h before the addition of C-R/T liposomes. The cells were incubated at the 37 or 4 °C for 4 h, then the cells were washed three times with cold PBS (pH 7.4) and fixed with 4% paraformaldehyde. The cell nuclei were stained with DAPI for 5 min followed by another wash with PBS for 3 times. Coverslips were mounted cell-side down with slides and viewed using a Leica TCS SP5 AOBS confocal microscopy system.

2.8. Intracellular fate of liposomes

HepG2 cells were seeded on coverslips at a density of 2.5×10^5 per well in a six-well plate. After 24 h cultivation, cells were incubated with CFPE-labeled liposomes for 4 h at 37 °C in the presence of 20 mM cysteine, and then incubated with LysoTracker Red (100 nM) for 1 h at the end of incubation. Then the cells were washed three times with cold PBS (pH 7.4), coverslips were mounted cell-side down with slides and viewed using a Leica TCS SP5 AOBS confocal microscopy system.

2.9. Upatake of liposomes by HepG2 spheroids

In vitro HepG2 spheroids were established using a lipid overlay system as reported previously (Gao et al., 2014a,b,c; Perche and Torchilin, 2012). Briefly, 2% (m/V) agarose was added into serum-free 1640 culture medium and heated to 80 °C for 30 min. 50 μL of agarose solution was added to each well of a 96-well plate (Gao et al., 2012a,b). After the agarose solution was cooled to room temperature, HepG2 cells were seeded into each well at a density of 2×10^3 per well. After one week, the formed tumor spheroids were incubated with CFPE-labeled liposomes for 4 h at 37 °C, then the spheroids were washed three times with ice-cold PBS and fixed with 4% paraformaldehyde. Finally the spheroids were viewed using a Leica TCS SP5 AOBS confocal microscopy system (Leica, Germany).

2.10. In vivo *imaging of liposomes in HepG2-xenografted nude mice*

Nude mice weighing 20–25 g were purchased from Experiment Animal Center of Sichuan University (PR China). All the animal experiments adhered to the principles of care and use of laboratory animals and were approved by the Experiment Animal Administrative Committee of Sichuan University.

The DIR loaded liposomes (2 mg lipids/mL) were utilized to investigate the distribution of liposomes in nude mice bearing HepG2, human hepatocellular carcinoma. HepG2-xenografted nude mice were established as described previously (Kuai et al., 2010). Briefly, about 2×10^6 tumor cells were subcutaneously injected in the left flank of the nude mice. Tumors were allowed to grow to an average size of about 10 mm in diameter. Different formulations of DIR loaded liposomes were injected at a dose of 20 mg lipids/kg via the tail vein. Twenty-four hours after administration, PBS (pH 7.4) or cysteine in PBS (30 mg/mL) was injected via the tail vein at a dose of 4 mL/kg to evaluate the effect of cysteine on the delivery *in vivo*. Four hours after the injection, the *in vivo* fluorescence imaging was performed with an IVIS® Spectrum system (Caliper, Hopkington, MA). Then the nude mice were sacrificed and the fluorescence intensity of various organs was measured.

2.11. Distribution of liposomes in HepG2 tumor tissue

To investigate the distribution of liposomes in HepG2 tumor tissue, DID (an analogue of DIR)-loaded liposomes (2 mg lipids/mL) were administered into tumor-bearing mice as described above. Then the nude mice were sacrificed and tumors were excised and frozen sectioned (4 μm in thickness). Sections were stained with DAPI for 5 min, washed three times with cold PBS, and then observed using a Leica TCS SP5 AOBS confocal microscopy system.

2.12. Statistical analysis

Data were presented as means ± SDs unless particularly outlined. Statistical significances were determined using the Student's *t*-test. A P-value < 0.05 was considered to be significant, and a P-value < 0.01 was considered as highly significant.

3. Results and discussion

3.1. Characterization of materials

Time-of-flight electrospray mass spectrometry (TOF MS ES+) confirmed the formation of the synthesized materials, DSPE-PEG_{1000}-TAT (M_w calculated = 3820 Da, M_w observed = 3837 Da), DSPE-PEG_{3500}-RGD (M_w calculated = 5148 Da, M_w observed = 5146 Da), DSPE-S-S-PEG_{5000} (M_w calculated = 5800 Da, M_w observed = 5788 Da), DSPE-PEG_{5000}-OMe (M_w calculated = 5800 Da, M_w observed = 5806 Da) (see Supplementary Information Fig. S1).

3.2. Characteristics of liposomes

Liposome size measurements showed that the sizes of all formulations prepared in this study were within the range of 80–120 nm. The mean size of the liposomes increased slightly with the modification of single ligand or dual ligands, but decreased with the introduction of 8% PEG in the liposomes, which was

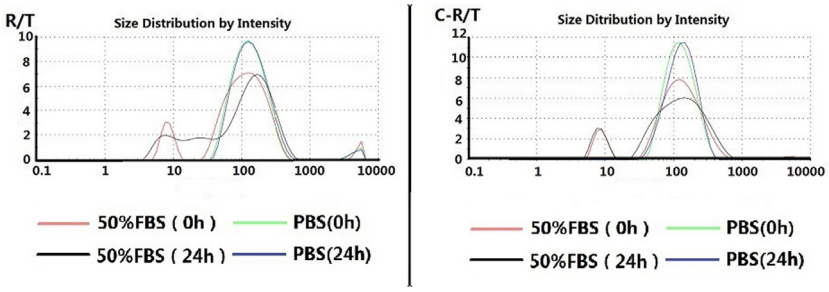

Fig. 2. Stability of liposomes after incubation in 50% FPS or PBS at 37 °C for 24 h.

consistent with the previous studies that the formation of a hydrophilic layer was an important factor in the formation of small, homogenous lipid particles (Masuda et al., 2009). According to the previous reports, when liposomes contained up to 4 mol% of PEG lipids, neighboring coils did not interact laterally thus creating a mushroom regime. As the proportion of PEG lipids in liposomes exceeded 4 mol%, neighboring PEG chains pushed against each other, and extended further out from the surface on which they are grafted, leading to the brush regime. As the amount of PEG lipids increased, the mushroom-brush phase transition started to take place, which resulted in a decrease in size (Garbuzenko et al., 2005). The zeta potential of liposomes changed slightly after the modification of DSPE-PEG$_{3500}$-RGD, DSPE-PEG$_{1000}$-TAT, DSPE-S-S-PEG$_{5000}$ and DSPE-PEG$_{5000}$-OMe. In addition, encapsulation of DIR or DID did not affect the size (data not shown). The morphological observation by TEM image revealed that the liposomes were homogeneously spheroids (as shown in Fig. S2).

3.3. Stability of liposomes in the presence of fetal bovine serum

Liposomes can bind to plasma proteins during the circulation and then be taken up by the RES, so the aggregation behavior of liposomes in the FBS can reflect the stability of the liposomes *in vivo*. To investigate the aggregation behavior of the R/T and C-R/T liposomes, their sizes were monitored by dynamic light scattering (DLS) in PBS (pH 7.4) and 50% FBS. No increase in size after 24 h in PBS for R/T liposomes, but when the same DLS measurements were conducted in 50% FBS, the size of R/T liposomes increased markedly which indicated the aggregation of liposomes. On the other hand, C-R/T liposomes did not increase in size at all after 24 h both in PBS and in FBS (Fig. 2). These results indicated that the stability of liposomes was enhanced because the PEGylation formed an aqueous layer on the surface of liposomes which suppressed the direct interactions between carrier and plasma proteins, providing support for the extended circulation time of the liposomes *in vivo* (Hansen et al., 2012; Hatakeyama et al., 2007a,b).

3.4. In vitro *cellular uptake*

In order to see if dual ligands could be efficiently shielded by cleavable PEG and to investigate the level of exposure of dual ligands by cysteine, various amounts of cleavable PEG were incorporated into the formulation of liposomes. As shown in Fig. 3A, the cellular uptake decreased gradually with the density of cleavable PEG in liposomes increasing from 2% to 10% and significantly increased in the presence of 20 mM cysteine ($P < 0.001$), which was due to the steric hindrance effect of PEG (Hatakeyama et al., 2009). The amount of uptake reached a platform when the liposomes were modified with 8% DSPE-S-S-PEG$_{5000}$, and the shielding effect would not be further enhanced with the increase of DSPE-S-S-PEG$_{5000}$ proportion. These results indicated that dual ligands could be well masked by 8% DSPE-S-S-PEG$_{5000}$ and could be sufficiently exposed in the presence of 20 mM cysteine. As a result, the optimal density of cleavable PEG on the liposomes was determined to be 8% (molar ratio). Moreover, the uptake efficiency decreased gradually with the increase of the molar ratios of DSPE-S-S-PEG$_{5000}$ after giving 20 mM cysteine implying that the cleavable PEG could not be entirely detached from the liposomes in the presence of 20 mM cysteine. Dual ligands should have been fully exposed due to the cleavage of disulfide bonds and the detachment of the "shielding" PEG block. However, the cleavage is a time-dependent kinetic reaction and the cellular uptake is also a time-dependent process, therefore the disulfide bonds may not have been completely cleaved after incubation for 4 h (Koren et al., 2012). On the other hand, we examined the cleavage of DSPE-S-S-PEG5000 with various

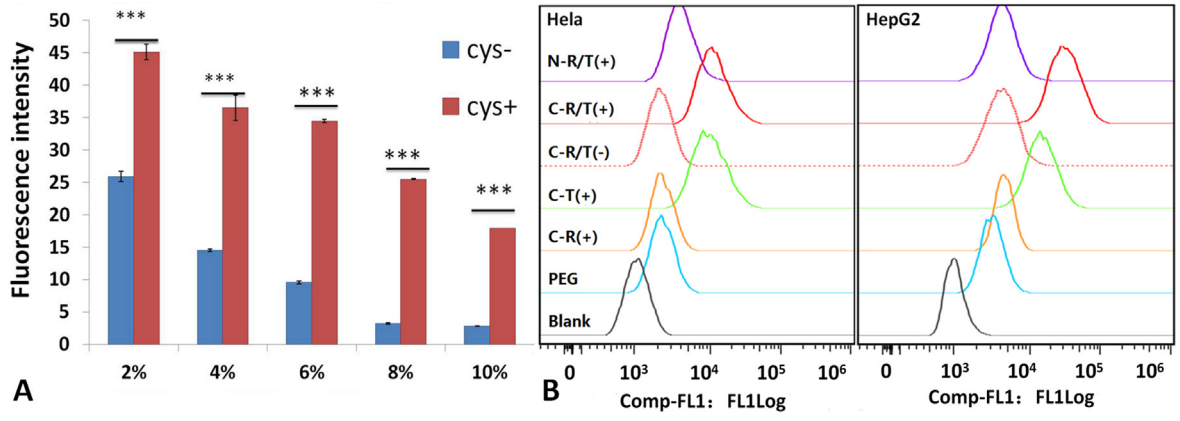

Fig. 3. Cellular uptake of liposomes modified with different amounts of cleavable PEG in HepG2 cell (A), $^{*}P < 0.05$, $^{**}P < 0.01$, $^{***}P < 0.001$. Uptake of liposomes in Hela and HepG2 cell with (+) or without (−) cysteine (B).

concentrations of cysteine, and 20 mM cysteine which had adequate cleaving capacity and low toxicity was chosen for the follow-up test (data not shown). A L-Cys concentration higher than 20 mM was not suitable for this study because some potential toxic side effects might be caused at higher concentration. Appropriate PEG chain lengths and the percentages of ligands included in each liposomal formulation also needed to be considered, because these parameters greatly affected the shielding capability of cleavable PEG and the synergistic effect of RGD and TAT. After a series of screening tests, 8% DSPE-S-S-PEG_{5000} was utilized to mask 1% DSPE-PEG_{3500}-RGD and 0.5% DSPE-PEG_{1000}-TAT (data not shown).

Hela cells were selected as a tumor cell type with relatively low expression of integrin receptors while HepG2 cells were known to be overexpressed with integrin receptors (Borgne-Sanchez et al., 2007; Li et al., 2011). To investigate the selectivity and internalization of multistage liposomes, the cellular uptake of different liposomes in Hela and HepG2 cells was examined, as shown in Fig. 3B. There was no significant difference between the cellular uptake of PEG liposomes and RGD liposomes in both cells, and in Hela cells the C-R/T liposomes showed minor improvement in the cellular uptake compared with C-T liposomes in the presence of cysteine. However, in HepG2 cells the RGD modification stimulated the uptake by 2-fold compared with the PEG liposomes, and the uptake of C-R/T liposomes with cysteine increased 4-fold compared with the C-T liposomes with cysteine. The cellular uptake results were consistent with the integrin expression levels on cell surface, indicating that the RGD motif had the ability to recognize and target integrin receptors expressed on the surface of cells. Moreover, the modification of TAT exhibited a synergistic effect with RGD on the cellular uptake of liposomes in integrin expressing cells, suggesting that after the recognition of integrins by the RGD motif, the TAT could further enhance the internalization of liposomes. At the same time, C-R/T liposomes displayed more efficient intracellular delivery in the presence of cysteine while N-R/T liposomes showed no significant enhancement with cysteine, suggesting that the dual ligands were exposed after PEG detaching and allowed liposomes to interact more efficiently with cells.

The cellular uptake of liposomes was further studied by confocal microscopy. As shown in Fig. 4,the cellular uptake of PEG liposomes was set as a control. Compared to the control, the RGD liposomes showed a very weak fluorescence signal in both Hela and HepG2 cells, indicating that the RGD-mediated cellular uptake was quite limited. In contrast, much higher cellular uptake was observed for the TAT liposomes in both Hela and HepG2 cells, suggesting that cell-penetrating peptide TAT had the ability to mediate non-selective cellular uptake of liposomes. The cellular uptake of mixed RGD liposomes and TAT liposomes (R + T) showed a superposition of the effect of RGD liposomes and TAT liposomes, suggesting that only the mixing of two single-ligand liposomes had no synergistic effect. The dual-ligand liposomes (R/T) showed similar fluorescence intensity with the TAT liposomes in Hela cells, while the R/T liposomes resulted in stronger fluorescence signals than the TAT liposomes in HepG2 cells, indicating that the dual ligands exhibited a synergistic effect on the cellular uptake of liposomes in integrin expressing cells. These results proved that the synergistic effect of the dual-ligand liposomes was related to the conformation of the two ligands (Kluza et al., 2010). At the same time, we can also see that the dual ligands can be fully shielded by cleavable PEG and exposed in the presence of 20 mM cysteine.

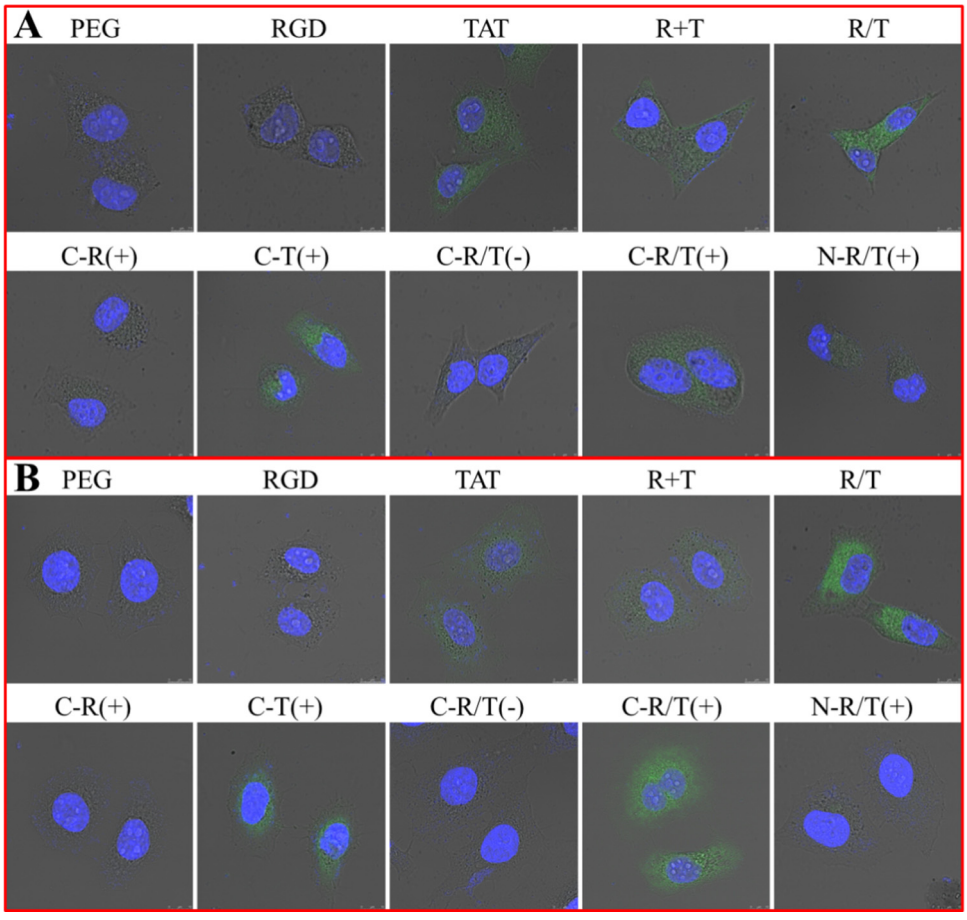

Fig. 4. Uptake of liposomes in Hela (A) and HepG2 (B) with (+) or without (−) cysteine observed by CLSM.

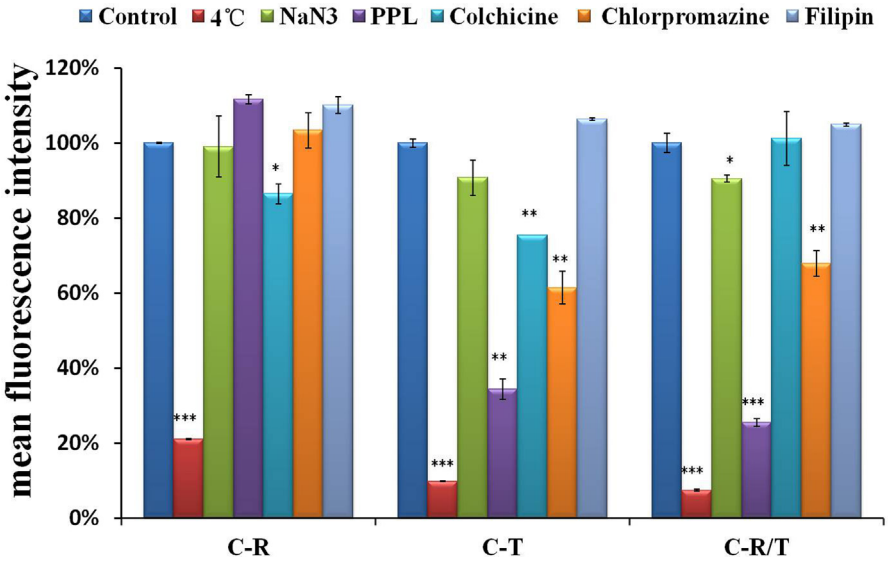

Fig. 5. Effects of endoeytosis inhibitors on the cellular uptake of liposomes in HepG2. The data are presented as the mean ± SD ($n = 3$), $^{*}P < 0.05$, $^{**}P < 0.01$, $^{***}P < 0.001$.

The results of quantitative and qualitative analysis of cellular uptake showed that the multistage liposomes (C-R/T) had better cell selectivity and stronger internalization than other liposomes in the presence of L-cysteine. The C-R/T liposomes could specifically recognize cells overexpressing integrins and mediate efficient internalization in the synergistic effect of the RGD and TAT after the detachment of the cleavable PEG.

3.5. Cellular uptake mechanism of modified liposomes in HepG2

To determine the possible involvement of different endocytic pathways in the cellular uptake of liposomes in HepG2 cells, several classical inhibitors of endocytosis were used, and the fluorescence of cells treated with the different liposomal formulations without any inhibitor was set as 100% and as the control. As shown in Fig. 5, the uptake of C-R, C-T and C-R/T liposomes was decreased by about 80%, 90% and 93% ($P < 0.001$) in comparison to control at 4 °C due to the down-regulated cell metabolism, implying that the cellular uptake of liposomes was depended on temperature. Treatment of cells with the energy inhibitor NaN_3 did not significantly change the cellular uptake of C-R liposomes, however, the cellular uptake of C-T and C-R/T liposomes was decreased by about 10% ($P < 0.05$), indicating that the cellular uptake of C-T and C-R/T liposomes was dependent on energy.65% ($P < 0.01$) and 70% ($P < 0.001$) decrease in cellular uptake of C-T and C-R/T liposomes was observed after incubation in the presence of poly-L-lysine (PPL), which was a positively charged amino acid polymer that had the ability to bind with the negatively charged cell membrane, suggesting that the uptake of C-T and C-R/T liposomes was influenced by the charges of liposomes. It was reported that the TAT sequence contained many basic amino acids which had strong cationic properties, so electrostatic interactions could be generated between TAT and the negatively charged cell membrane. Therefore, the cellular uptake of the C-R/T liposomes was mainly influenced by the cationic nature of the TAT motif. The uptake of C-R and C-T liposomes was decreased by about 10% ($P < 0.05$) and 20% ($P < 0.01$) after incubation with colchicine. Colchicine was known to inhibit the formation of microfilaments and microtubule, therefore, it had an effect on macropinocytosis-mediated uptake. The small effect of colchicine on the uptake of C-R and C-T liposomes showed that macropinocytosis was presumably involved to a lesser extent. At the same time, by preventing the recycling of clathrin and hindering endocytosis through clathrin-dependent mechanisms with the cationic amphiphilic drug chlorpromazine, a significant decrease (40% and 35% $P < 0.01$) in cellular uptake of C-T and C-R/T liposomes was observed in the presence of chlorpromazine, suggesting that the clathrin-dependent pathway was involved in the internalization of C-T and C-R/T liposomes. The cellular uptake of all liposomes did not significantly change with the caveolae-dependent endocytosis inhibitor filipin. These results suggested that the cellular uptake of these liposomes was determined by the combination of various endocytic pathways (Kibria et al., 2011).

Interestingly, the cellular uptake mechanism of C-R/T liposomes was similar to the C-T liposomes, indicating that the TAT dominated in the cellular uptake process of the C-R/T liposomes, which was consistent with our expectations. Meanwhile, the cellular uptake mechanism of the C-R/T and C-T liposomes was not exactly the same, suggesting that the C-R/T liposomes may produce a new mechanism on the basis of the C-T liposomes.

3.6. The binding and internalization of C-R/T liposomes in HepG2 in the presence of free RGD

To evaluate the binding and internalization of CFPE-labeled C-R/T liposomes (20 μg/mL) in HepG2 cells in the presence of free RGD, the cell uptake was observed at different temperatures. As shown in Fig. 6, at 37 °C the fluorescence signals were almost all within the cells and around the cell nuclei while the fluorescence signals were mostly seen on cell surfaces at 4 °C, which was consistent with Fig. 5, suggesting that the internalization of C-R/T liposomes was a temperature-dependent process and the C-R/T liposomes just bound to cells without uptake into cells at 4 °C (Song et al., 2009). In addition, free RGD significantly inhibited the binding of C-R/T liposomes at 4 °C but almost did not affect the internalization of liposomes at 37 °C. These results indicated that the RGD motif was mainly involved in the cellular binding rather than internalization of the C-R/T liposomes and there might be another uptake pathway mediated by TAT after the binding of RGD to integrins (Kibria et al., 2011). These results were consistent with the purpose of the experimental design that the outer RGD was exposed after the detachment of PEG, then recognized and bound to integrin

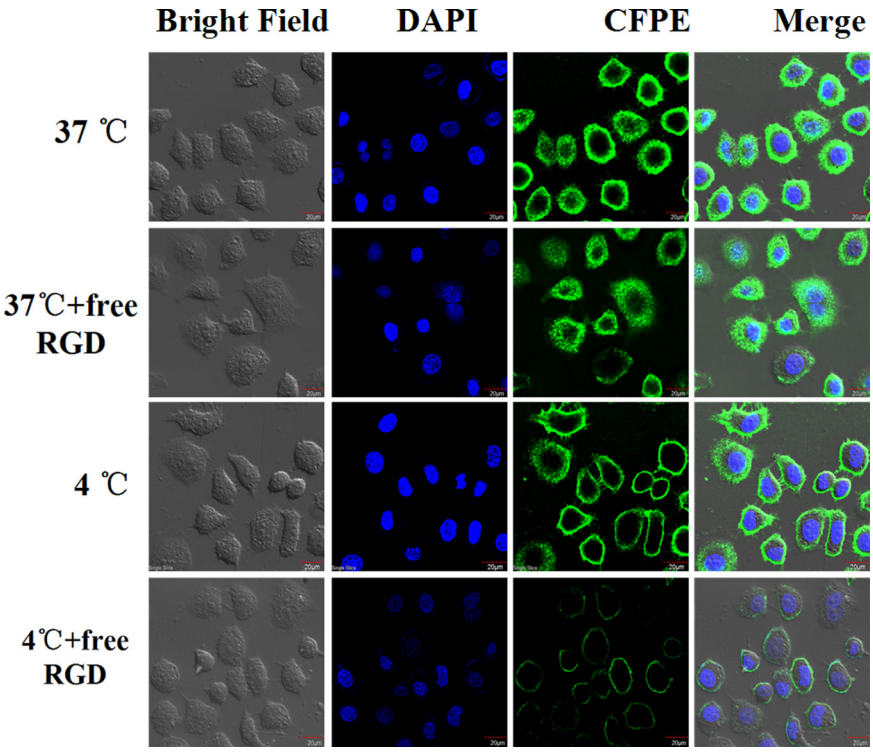

Fig. 6. The cellular uptake of C-R/T liposomes in HepG2 cells at 4 or 37 °C in the presence of 50 mol excess free RGD.

receptors on the cell surface which narrowed the distance between liposomes and cells, and the liposomes were internalized into cells by the synergistic effect of RGD and TAT.

3.7. Intracellular fate of liposomes

To further investigate the cell trafficking of the liposomes, the late endosomes and the lysosomes were stained by LysoTracker Red, a well-known marker for acidic intracellular vesicles. Fig. 7 showed that almost all C-R liposomes were distributed in acidic compartments of the cells, as revealed by the appearance of numbers of yellow dots (merged colors of CFPE and LysoTracker RED) in the images. On the other hand, a large fraction of the C-T liposomes appeared in the cytoplasmic region outside lysosomes. Meanwhile, the C-R/T liposomes were mainly distributed in the cytoplasm but some of them still existed in the lysosomes. It was

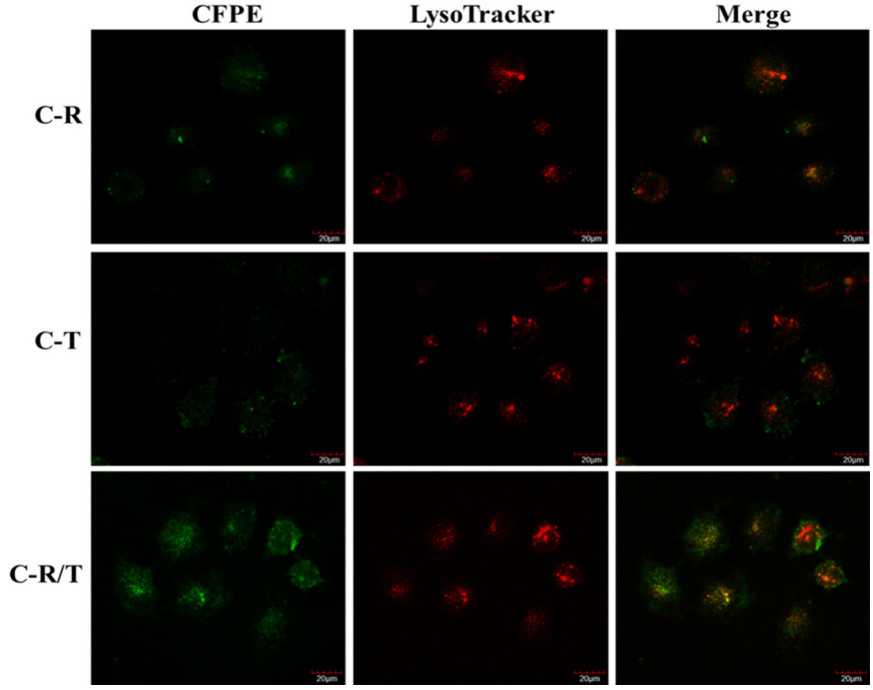

Fig. 7. Intracellular localization of C-R, C-T and C-R/T liposomes in HepG2 cells, as determined by CLSM, green (CFPE), red (LysoTracker), yellow (colocalized CFPE and LysoTracker).

worth mentioning that the cellular uptake of C-T and C-R/T liposomes was mainly clathrin-mediated endocytosis, which meant that exogenous substances eventually reached lysosomes via early endosomes and late endosomes after being taken up into the cells (Pelkmans and Helenius, 2002). However, the C-T and C-R/T liposomes were mainly distributed in the cytoplasmic region outside lysosomes, indicating that the C-T and C-R/T liposomes had the ability to escape from the lysosomes into the cytoplasm after internalization of the lysosomes. These results suggested that the excess cleavable PEG which did not entirely shed from the liposome surface further detached under the reducing action of the enzyme in the lysosome, reducing the stability of liposomes to enhance the fusion ability of the liposomes with the lysosome membrane, then liposomes escaped from the lysosomes owing to the membrane fusion effect of TAT (Xiong and Lavasanifar, 2011). The uptake mechanism successfully avoided the degradation of lysosomes, providing a possibility for the delivery of gene into cells.

The results of cellular uptake mechanism and intracellular fate showed the intracellular delivery process of the C-R/T liposomes. The C-R/T liposomes recognized and bound to integrin receptors via the RGD ligand after the cleavage of PEG by cysteine, and the uptake was mainly relied on the electrostatic interaction of TAT ligand with negatively charged cell surface. The stability of liposomes significantly reduced with the further detachment of the cleavable PEG residues in the presence of the reductive lysosomal enzyme, and the liposomes escaped from the lysosomes with the help of the membrane fusion effect of TAT. Although the uptake mechanisms and intracellular trafficking of CPPs-modified drug delivery systems have been widely studied in the past, researches about the mechanisms of multistage liposome systems have rarely been reported (Kale and Torchilin, 2007; Kuai et al., 2011).

3.8. Uptake of liposomes by HepG2 spheroids

For evaluating the effects of the solid tumor penetration of the multistage liposomes *in vitro*, multicellular 3D tumor spheroids which have been proposed as models of intermediate complexity between monolayer cultures and xenografts because of their similarities to *in vivo* avascular tumor tissues (Gao et al., 2012a,b; Jiang et al., 2013) were observed by confocal microscopy. As shown in Fig. 8, the PEG liposomes almost entirely lacked efficient penetrating on HepG2 spheroids and the C-R liposomes in the presence of cysteine showed much weaker fluorescence, indicating that the liposomes without modification or modified with specific molecule (RGD) had very weak penetration. For the C-T liposomes in the presence of cysteine, much higher fluorescence was observed primarily on the periphery of tumor spheroids, but it did not penetrate into the core of the HepG2 tumor spheroids. However, an apparent enhanced fluorescence of the C-R/T liposomes was observed in the presence of cysteine, and the fluorescence could be observed as deep as 105 μm within, suggesting that solid tumor penetration was enhanced by the synergistic effect of RGD and TAT. It was worth mentioning that the penetration ability of the C-R/T liposomes was weaker than that of the R/T liposomes, this may be due to the incomplete detachment of cleavable PEG. Meanwhile, the fluorescence of C-R/T liposomes without Cys and the fluorescence of N-R/T liposomes with Cys on HepG2 tumor spheroids were hardly visible, indicating that the dual ligands could only produce

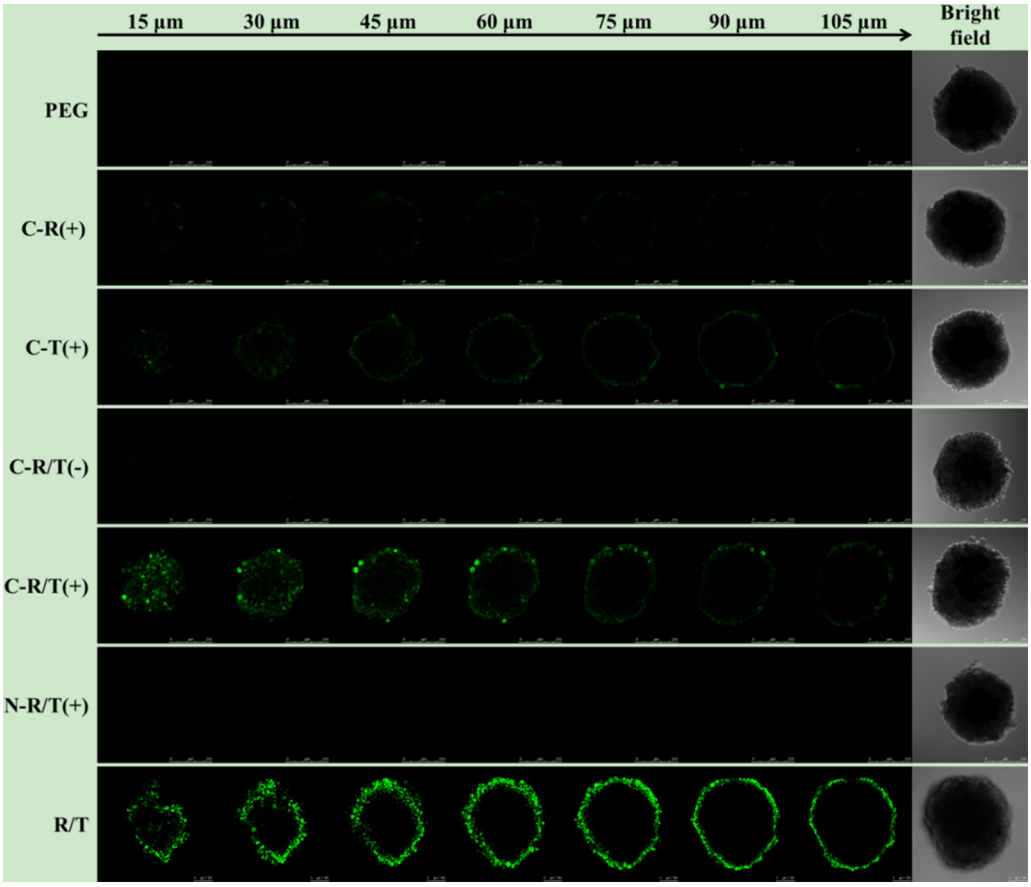

Fig. 8. Penetration of CFPE-labeled liposomes throughout HepG2 spheroids. Z-stack images were obtained from the top toward the tumor spheroid equatorial plane in 15 μm intervals. The scale bar represents 250 μm.

synergistic effect after the removal of PEG. These results were consistent with the cellular uptake of monolayer cells, suggesting that the synergistic effect of dual ligands not only enhanced the uptake of monolayer cells but also promoted the deeper penetration into the avascular tumor tissues. Chemotherapeutic effect of solid tumors is often compromised due to several physiologic barriers which significantly limit the penetration of anticancer drugs into neoplastic cells distant from blood vessels (Cairns et al., 2006; Gao et al., 2013a,b). The system successfully promoted a deeper penetration into the avascular tumor tissues, providing a promising strategy for improving the treatment.

3.9. In vivo *imaging of liposomes in HepG2-xenografted nude mice*

The *in vivo* biodistribution and tumor accumulation profiles of DIR-loaded liposomes were clearly visualized by monitoring the whole body NIRF intensity in subcutaneous xenograft bearing nude mice model (Fig. 9A). The NIR fluorescence intensities in the tumor region of all liposomes modified with 8% PEG(C-R (+), C-T (+), C-R/T (−), C-R/T (+) and N-R/T (+) were strong and the strength was substantially similar, which verified the ability of cleavable PEG to mask targeting ligands on liposomes to evade the RES and accumulate in tumor region via EPR effect after intravenous

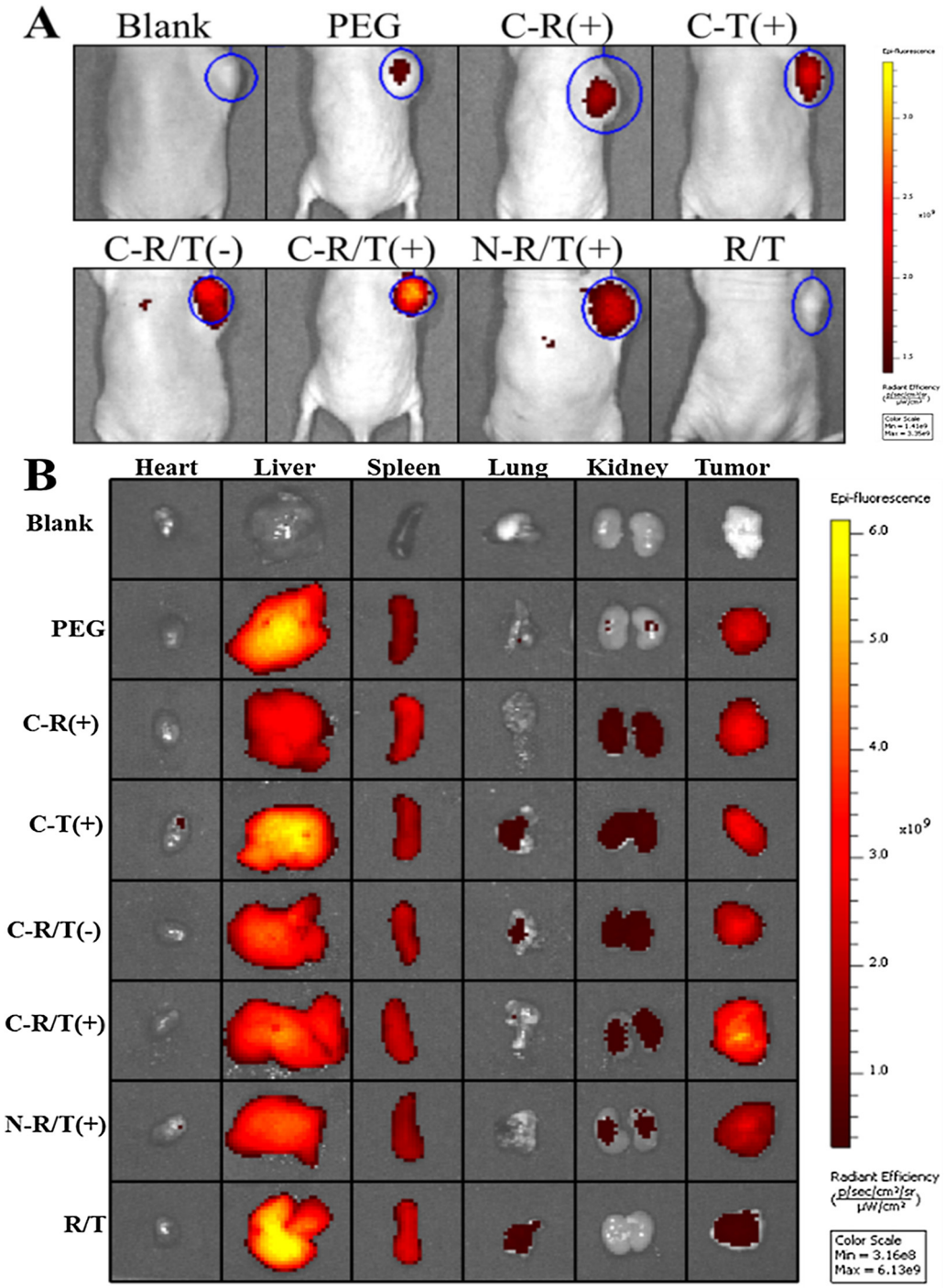

Fig. 9. *In vivo* fluorescence imaging of HepG2-xenografted nude mice after injection of DIR-labeled liposomes (A). Representative images of dissected organs of tumor-bearing nude mice sacrificed post intravenous injection of DIR-labeled liposomes (B).

administration. We can also observe that the NIR fluorescence intensities in the tumor region of the C-R/T liposomes slightly enhanced with the intravenous injection of cysteine. The result implied that after the C-R/T liposomes reached the tumor site, the thiolytic cleavage of some PEG-S-S chains took place in response to exogenous administration of L-cysteine, resulting in the exposure of the dual ligands, which further enhanced the accumulation of C-R/T liposomes in the tumor tissue. However, the R/T liposomes without the modification of PEG showed almost no accumulation at the tumor site, while there was a certain accumulation of PEG liposomes, implying that the C-R/T liposomes without the protection of PEG were taken up by the RES quickly.

Four hours after intravenous injection of cysteine, the tumor-bearing mice were sacrificed, and major organs and tumor tissues were isolated and observed (Fig. 9B). The tumor accumulation of liposomes was consistent with the results of the *in vivo* images. Obviously, the tumor accumulation was the highest for C-R/T (+) liposomes. These results implied that the C-R/T (+) liposomes could efficiently target to solid tumors and decrease non-specific accumulation in normal organs such as livers, lungs and kidneys. The fluorescence signals of PEG, C-T (+) and R/T liposomes in liver were higher than other liposomes, implying that the RES had the strongest capturing capability for these liposomes. The proportion of PEG lipids was low for the PEG liposomes, which has a shorter circulation time leading to the RES capture, and for the C-T liposomes, after the PEG cleavage of the C-T liposomes, the TAT ligand of liposomes was exposed, and C-T liposomes in the blood circulation were captured by the RES due to the positive charge of the TAT. The R/T liposomes without the protection of PEG could be taken up by the RES quickly leading to higher distribution in livers. Moreover, C-T (+) and R/T liposomes also had some accumulation in the lung, which may be related to the positive charge of the TAT ligand. Preliminary studies have demonstrated that the passive accumulation of liposomes reached maximum in tumor tissue between 24 and 48 h (Maeda et al., 2009), and the half-life of 8% DSPE-S-S-PEG_{5000} modified liposomes *in vivo* was about 27 h (McNeeley et al., 2009), which provided sufficient time for liposomes to accumulate at the tumor site, therefore the cysteine was injected 24 h after the administration of liposomes.

The results of serum stability and biodistribution suggested that the cleavable PEG was capable of increasing the stability of liposomes and concealing dual ligands from the RES, and ultimately, the C-R/T liposomes obtained remarkable accumulation in the tumor region.

3.10. Distribution of liposomes in HepG2 tumor tissue

The *in vivo* solid tumor permeation and targeted delivery efficiency of DID labeled liposomes were studied qualitatively by confocal microscopy observation of the frozen sections of subcutaneous tumor. As shown in Fig. 10, for the PEG, N-R/T (+) and R/T liposomes, almost no red fluorescence signals were distributed in tumor tissue, implying that these liposomes could accumulate in the tumor area via the EPR effect but could not be effectively taken up into cells. The C-R (+) liposomes showed a slightly enhanced red fluorescence distribution, and the fluorescence uniformly dispersed in the tumor tissue. In contrary, the C-T (+) liposomes showed stronger and uneven distribution of fluorescence in the tumor tissue, indicating that the TAT may generate electrostatic interactions with negatively charged cell membrane, which could produce enhanced internalization, but it was easy to form a fluorescent precipitate on the cell surface. In addition, the C-R/T liposomes have almost no fluorescence signal without the intravenous injection of cysteine, but it showed strong

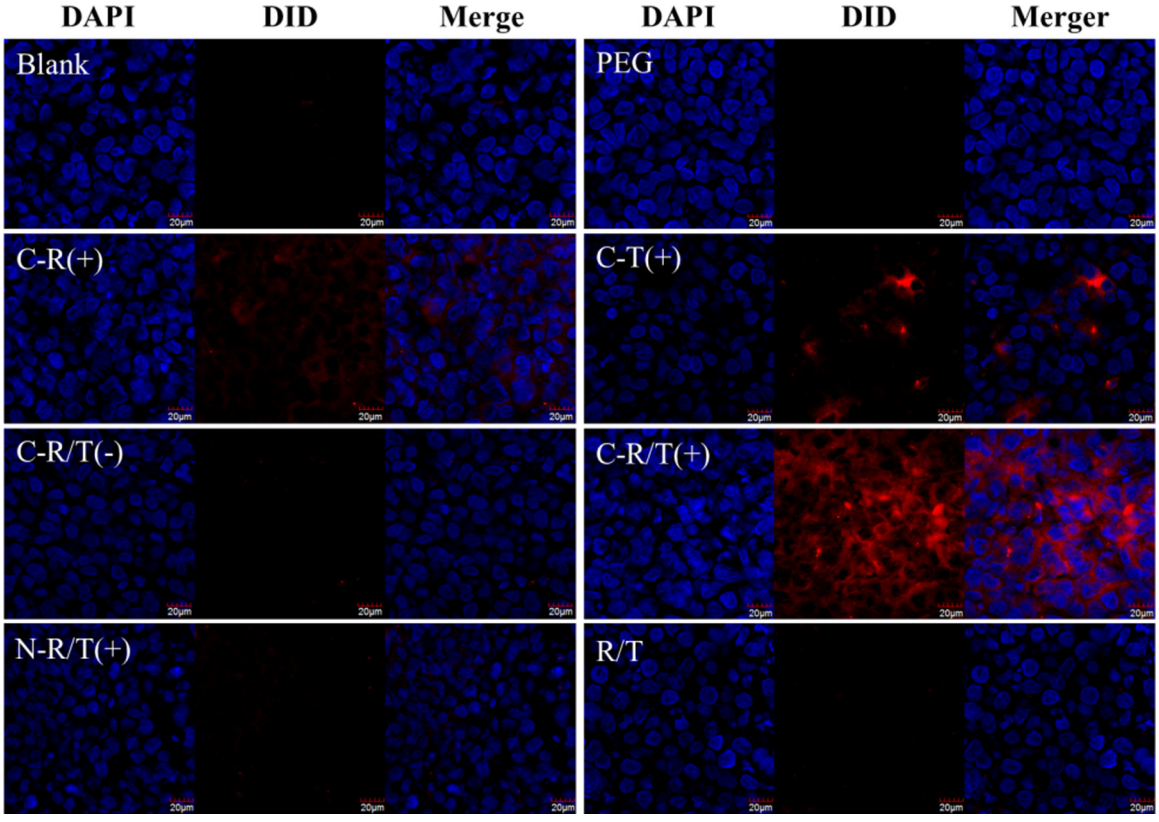

Fig. 10. CLSM images of HepG2 tumor frozen sections from tumor-bearing nude mice receiving various DID loaded liposomes.

and uniform red fluorescence after the injection of cysteine. Combining with the results of biodistribution, it could be concluded that liposomes modified with PEG could be effectively accumulated in solid tumor tissue, but the PEGylation hindered the further contact of liposomes with tumor cells (Kuai et al., 2011; McNeeley et al., 2009). However, the internalization of liposomes was significantly enhanced after the detachment of cleavable PEG via systemic administration of cysteine. Moreover, RGD and TAT in the C-R/T liposomes had a strong synergistic effect to promote liposomes to be taken up into the cells in the presence of cysteine which was consistent with the results of cellular uptake *in vitro*. The synergistic effect of C-R/T (+) liposomes promoted the internalization of liposomes at the tumor site, resulting in enhanced accumulation of C-R/T liposomes in the tumor tissue (as shown in Fig. 9). It was worth mentioning that the red fluorescence of C-T liposomes mainly distributed on the cell surface, but the fluorescence of C-R/T liposomes almost all located around the nuclei, indicating that although the cellular uptake of the C-R/T liposomes was mainly influenced by the cationic nature of the TAT motif, and the fluorescent precipitate formed by the positive charge may be avoided in the presence of RGD.

The cellular uptake *in vitro*, the tumor spheroids penetration and the distribution of liposomes in HepG2 tumor tissue all indicated that the liposomes modified with single ligand (no matter CPP or the specific ligand) had relatively weak capability to be taken up into cells, and the C-R/T liposomes could be efficiently internalized in the synergistic effect of RGD and TAT in the presence of cysteine.

Overall, the multistage liposomes (C-R/T) were more stable than the dual-ligand liposomes (R/T), and had much stronger internalization into cells over-expressing integrins than single-ligand liposomes (C-R and C-T) modified with cleavable in the presence of cysteine. These results strongly supported our hypothesis that the stability of multistage liposome system was increased by the protection of cleavable PEG_{5000} in the outermost layer, which can avoid the binding of ligands in the inner layer with plasma proteins. Upon reaching sufficient accumulation via the EPR effect in tumors, the shielding layer was detached and the dual ligands in the inner layer were exposed through exogenous administration of a safe reducing agent L-cysteine. The exposed dual ligands recognized the integrins, bound with the cell surface, and the liposomes were efficiently internalized into cells via a synergistic effect of RGD and TAT. Such an approach successfully avoided the capture of RES and resolved the PEG dilemma by modification of cleavable PEG_{5000}. Meanwhile, the multistage liposomes also enhanced the internalization of liposomes in the tumor tissues through the synergistic effect of RGD and TAT. However, tumor cells displayed their diversity because of various cell types, proteomics, genomics and many others (Bae, 2009). So for more efficient tumor therapy, it's worth further discussion about killing a fraction of the cell population which expresses enough specific receptors or killing all the cells in the tumor without selectively.

4. Conclusions

In the present study, we established a multistage delivery system modified with cleavable PEG, RGD and TAT, which combined the advantages of cleavable PEG, specific ligand and penetrating peptide. The multistage liposomes with three-tier cascade structure increased the stability of liposomes and showed synergistic effect of TAT and RGD. The system displayed excellent tumor targeting efficiency both *in vitro* and *in vivo*. Although it was a preliminary study, the results demonstrated a tremendous potential of this multistage liposomes for efficient delivery to tumor tissue and selective internalization into tumor cells.

Acknowledgments

We are thankful for the financial support of the National Natural Science Foundation of China (81072599) and the National Basic Research Program of China (2013CB932504).

Appendix A. Supplementary data

Supplementary data associated with this article can be found, in the online version, at http://dx.doi.org/10.1016/j.ijpharm.2014.04.008.

References

Bae, Y.H., 2009. Drug targeting and tumor heterogeneity. Journal of Controlled Release 133, 2–3.
Borgne-Sanchez, A., Dupont, S., Langonné, A., Baux, L., Lecoeur, H., Chauvier, D., Lassalle, M., Déas, O., Brière, J.J., Brabant, M., Roux, P., Péchoux, C., Briand, J.P., Hoebeke, J., Deniaud, A., Brenner, C., Rustin, P., Edelman, L., Rebouillat, D., Jacotot, E., 2007. Targeted Vpr-derived peptides reach mitochond riato induce apoptosis of a Vb3-expressing endothelial cells. Cell death & differentiation 14, 422–435.
Burks, S.R., Macedo, L.F., Barth, E.D., Tkaczuk, K.H., Martin, S.S., Rosen, G.M., Halpern, H. J., Brodie, A.M., Kao, J.P., 2010. Anti-HER2 immunoliposomes for selective delivery of electron paramagnetic resonance imaging probes to HER2-overexpressing breast tumor cells. Breast Cancer Research and Treatment 124, 12–31.
Cairns, R., Papandreou, I., Denko, N., 2006. Overcoming physiologic barriers to cancer treatment by molecularly targeting the tumor microenvironment. Molecular Cancer Research 4, 61–70.
Duchardt, F., Fotin-Mleczek, M., Schwarz, H., Fischer, R., Brock, R., 2007. A comprehensive model for the cellular uptake of cationic cell-penetrating peptides. Traffic 8, 848–866.
Gao, H., Qian, J., Cao, S., Yang, Z., Pang, Z., Pan, S., Fan, L., Xi, Z., Jiang, X., Zhang, Q., 2012a. Precise glioma targeting of and penetration by aptamer and peptide dual-functioned nanoparticles. Biomaterials 33, 5115–5123.
Gao, H., Qian, J., Yang, Z., Pang, Z., Xi, Z., Cao, S., Wang, Y., Pan, S., Zhang, S., Wang, W., Jiang, X., Zhang, Q., 2012b. Whole-cell SELEX aptamer-functionalised poly (ethyleneglycol)-poly(epsilon-caprolactone) nanoparticles for enhanced targeted glioblastoma therapy. Biomaterials 33, 6264–6272.
Gao, H., Yang, Z., Zhang, S., Cao, S., Pang, Z., Yang, X., Jiang, X., 2013a. Glioma-homing peptide with a cell-penetrating effect for targeting delivery with enhanced glioma localization, penetration and suppression of glioma growth. Journal of Controlled Release 172, 921–928.
Gao, W., Xiang, B., Meng, T.T., Liu, F., Qi, X.R., 2013b. Chemotherapeutic drug delivery to cancer cells using a combination of folate targeting and tumor microenvironment-sensitive polypeptides. Biomaterials 34, 4137–4149.
Gao, H., Xiong, Y., Zhang, S., Yang, Z., Cao, S., Jiang, X., 2014a. RGD and interleukin-13 peptide functionalized nanoparticles for enhanced glioblastoma cells and neovasculature dual targeting delivery and elevated tumor penetration. Molecular Pharmacology 11, 1042–1052.
Gao, H., Yang, Z., Cao, S., Xiong, Y., Zhang, S., Pang, Z., Jiang, X., 2014b. Tumor cells and neovasculature dual targeting delivery for glioblastoma treatment. Biomaterials 35, 2374–2382.
Gao, H., Yang, Z., Zhang, S., Pang, Z., Liu, Q., Jiang, X., 2014c. Study of the pharmacology mechanisms of dual targeting drug delivery system with tumor microenvironment assays. Acta Biomaterialia 10, 858–867.
Garbuzenko, O., Barenholz, Y., Priev, A., 2005. Effect of grafted PEG on liposome size and on compressibility and packing of lipid bilayer. Chemistry and Physics of Lipids 135, 117–129.
Gullotti, E., Yeo, Y., 2009. Extracellularly activated nanocarriers: a new paradigm of tumor targeted drug delivery. Molecular Pharmacology 6, 1041–1051.
Hansen, M.B., van Gaal, E., Minten, I., Storm, G., van Hest, J.C., Löwik, D.W., 2012. Constrained and UV-activatable cell-penetrating peptides for intracellular delivery of liposomes. Journal of Controlled Release 164, 87–94.
Harding, J.A., Engbers, C.M., Newman, M.S., Goldstein, N.I., Zalipsky, S., 1997. Immunogenicity and pharmacokinetic attributes of poly(ethylene glycol)-grafted immunoliposomes. Biochimica et Biophysica Acta 1327, 181–192.
Hatakeyama, H., Akita, H., Ishida, E., Hashimoto, K., Kobayashi, H., Aoki, T., Yasuda, J., Obata, K., Kikuchi, H., Ishida, T., Kiwada, H., Harashima, H., 2007a. Tumor targeting of doxorubicin by anti-MT1-MMP antibody-modified PEG liposomes. International Journal of Pharmaceutics 342, 194–200.
Hatakeyama, H., Akita, H., Kogure, K., Oishi, M., Nagasaki, Y., Kihira, Y., Ueno, M., Kobayashi, H., Kikuchi, H., Harashima, H., 2007b. Development of a novel systemic gene delivery system for cancer therapy with a tumor-specific cleavable PEG-lipid. Gene Therapy 14, 68–77.
Hatakeyama, H., Ito, E., Akita, H., Oishi, M., Nagasaki, Y., Futaki, S., Harashima, H., 2009. A pH-sensitive fusogenic peptide facilitates endosomal escape and greatly enhances the gene silencing of siRNA-containing nanoparticles *in vitro* and *in vivo*. Journal of Controlled Release 139, 127–132.
Jiang, X., Xin, H., Gu, J., Xu, X., Xia, W., Chen, S., Xie, Y., Chen, L., Chen, Y., Sha, X., Fang, X., 2013. Solid tumor penetration by integrin-mediated pegylated poly(trimethylene carbonate) nanoparticles loaded with paclitaxel. Biomaterials 34, 1739–1746.

Kaasgaard, T., Mouritsen, O.G., Jørgensen, K., 2001. Screening effect of PEG on avidin binding to liposome surface receptors. International Journal of Pharmaceutics 214, 63–65.
Kale, A.A., Torchilin, V.P., 2007. Enhanced transfection of tumor cells invivo using "Smart" pH-sensitive TAT-modified pegylated liposomes. Journal of Drug Targeting 15, 538–545.
Khalil, I.A., Kogure, K., Akita, H., Harashima, H., 2006. Uptake pathways and subsequent intracellular trafficking in nonviral gene delivery. Pharmacological Reviews 58, 32–45.
Kibria, G., Hatakeyama, H., Ohga, N., Hida, K., Harashima, H., 2011. Dual-ligand modification of PEGylated liposomes shows better cell selectivity and efficient gene delivery. Journal of Controlled Release 153, 141–148.
Klibanov, A.L., Maruyama, K., Torchilin, V.P., Huang, L., 1990. Amphipathic polyethyleneglycols effectively prolong the circulation time of liposomes. FEBS Letters 268, 235–237.
Kluza, E., van der Schaft, D.W., Hautvast, P.A., Mulder, W.J., Mayo, K.H., Griffioen, A. W., Strijkers, G.J., Nicolay, K., 2010. Synergistic targeting of alphavbeta3 integrin and galectin-1 with heteromultivalent paramagnetic liposomes for combined MR imaging and treatment of angiogenesis. Nano Letters 10, 52–58.
Koren, E., Apte, A., Jani, A., Torchilin, V.P., 2012. Multifunctional PEGylated 2C5-immunoliposomes containing pH-sensitive bonds and TAT peptide for enhanced tumor cell internalization and cytotoxicity. Journal of Controlled Release 160, 264–273.
Kuai, R., Yuan, W., Qin, Y., Chen, H., Tang, J., Yuan, M., Zhang, Z., He, Q., 2010. Efficient delivery of payload into tumor cells in a controlled manner by TAT and thiolytic cleavable PEG co-modified liposomes. Molecular Pharmacology 7, 1816–1826.
Kuai, R., Yuan, W., Li, W., Qin, Y., Tang, J., Yuan, M., Fu, L., Ran, R., Zhang, Z., He, Q., 2011. Targeted delivery of cargoes into a murine solid tumor by a cell-penetrating peptide and cleavable poly(ethylene glycol) comodified liposomal delivery system via systemic administration. Molecular Pharmacology 8, 2151–2161.
Li, S., Wei, J., Yuan, L., Sun, H., Liu, Y., Zhang, Y., Li, J., Liu, X., 2011. RGD-modified endostatin peptide 30 derived from endostatin suppresses invasion and migration of HepG2 cells through the αvβ3 pathway. Cancer Biotherapy and Radiopharmaceuticals 26, 529–538.
Li, Y., He, H., Jia, X., Lu, W.L., Lou, J., Wei, Y., 2012. A dual-targeting nanocarrier based on poly(amidoamine) dendrimers conjugated with transferrin and tamoxifen for treating brain gliomas. Biomaterials 33, 3899–3908.
Maeda, H., Bharate, G.Y., Daruwalla, J., 2009. Polymeric drugs for efficient tumor-targeted drug delivery based on EPR-effect. European Journal of Pharmaceutics and Biopharmaceutics 71, 409–419.
Maeda, H., 2012. Macromolecular therapeutics in cancer treatment: the EPR effect and beyond. Journal of Controlled Release 164, 138–144.
Marcucci, F., Lefoulon, F., 2004. Active targeting with particulate drug carriers in tumor therapy: fundamentals and recent progress. Drug Discovery Today 9, 219–228.
Masuda, T., Akita, H., Niikura, K., Nishio, T., Ukawa, M., Enoto, K., Danev, R., Nagayama, K., Ijiro, K., Harashima, H., 2009. Envelope-type lipid nanoparticles incorporating a short PEG-lipid conjugate for improved control of intracellular trafficking and transgene transcription. Biomaterials 30, 4806–4814.
Matteo, P., Curnis, F., Longhi, R., Colombo, G., Sacchi, A., Crippa, L., Protti, M.P., Ponzoni, M., Toma, S., Corti, A., 2006. Immunogenic and structural properties of the Asn-Gly-Arg (NGR) tumor neovasculature-homing motif. Molecular Immunology 43, 1509–1518.
McNeeley, K.M., Annapragada, A., Bellamkonda, R.V., 2007. Decreased circulation time offsets increased efficacy of PEGylated nanocarriers targeting folate receptors of glioma. Nanotechnology 18, 385101.
McNeeley, K.M., Karathanasis, E., Annapragada, A.V., Bellamkonda, R.V., 2009. Masking and triggered unmasking of targeting ligands on nanocarriers to improve drug delivery to brain tumors. Biomaterials 30, 3986–3995.
Oba, M., Fukushima, S., Kanayama, N., Aoyagi, K., Nishiyama, N., Koyama, H., Kataoka, K., 2007. Cyclic RGD peptide-conjugated polyplex micelles as a targetable gene delivery system directed to cell spossessing alphavbeta3 and alphavbeta5 integrins. Bioconjugate Chemistry 18, 1415–1423.
Pappalardo, J.S., Quattrocchi, V., Langellotti, C., Giacomo, S., Gnazzo, V., Olivera, V., Calamante, G., Zamorano, P.I., Levchenko, T.S., Torchilin, V.P., 2009. Improved transfection of spleen-derived antigenpresenting cells in culture using TATp-liposomes. Journal of Controlled Release 134, 41–46.
Pelkmans, L., Helenius, A., 2002. Endocytosis via caveolae. Traffic 3, 311–320.
Perche, F., Torchilin, V.P., 2012. Cancer cell spheroids as a model to evaluate chemotherapy protocols. Cancer Biology and Therapy 13, 1205–1213.
Sapra, P., Tyagi, P., Allen, T.M., 2005. Ligand-targeted liposomes for cancer treatment. Current Drug Delivery 2, 369–381.
Sawant, R., Hurley, J.P., Salmaso, S., Kale, A., Tolcheva, E., Levchenko, T.S., Torchilin, V. P., 2006. "SMART" drug delivery systems: double-targeted pH-responsive pharmaceutical nanocarriers. Bioconjugate Chemistry 17, 943–949.
Schiffelers, R.M., Koning, G.A., Hagen, T.L., Fens, M.H., Schraa, A.J., Janssen, A.P., Kok, R.J., Molema, G., Storm, G., 2003. Anti-tumor efficacy of tumor vasculature-targeted liposomal doxorubicin. Journal of Controlled Release 91, 115–122.
Song, S., Liu, D., Peng, J., Deng, H., Guo, Y., Xu, L.X., Miller, A.D., Xu, Y., 2009. Novel peptide ligand directs liposomes toward EGF-R high-expressing cancer cells *in vitro* and *in vivo*. FASEB Journal 23, 1396–1404.
Takara, K., Hatakeyama, H., Kibria, G., Ohga, N., Hida, K., Harashima, H., 2012. Size-controlled, dual-ligand modified liposomes that target the tumor vasculature show promise for use in drug-resistant cancer therapy. Journal of Controlled Release 162, 225–232.
Terada, T., Iwai, M., Kawakami, S., Yamashita, F., Hashida, M., 2006. Novel PEG-matrix metalloproteinase-2 cleavable peptide-lipid containing galactosylated liposomes for hepatocellular carcinomaselective targeting. Journal of Controlled Release 111, 333–342.
Torchilin, V.P., 2008. Tat peptide-mediated intracellular delivery of pharmaceutical nanocarriers. Advanced Drug Delivery Reviews 60, 548–558.
Wu, Y., Chen, W., Meng, F., Wang, Z., Cheng, R., Deng, C., Liu, H., Zhong, Z., 2012. Core-crosslinked pH-sensitive degradable micelles: a promising approach to resolve the extracellular stability versus intracellular drug release dilemma. Journal of Controlled Release 164, 338–345.
Xiong, X.B., Huang, Y., Lu, W.L., Zhang, X., Zhang, H., Nagai, T., Zhang, Q., 2005. Enhanced intracellular delivery and improved antitumor efficacy of doxorubicin by sterically stabilized liposomes modified with a synthetic RGD mimetic. Journal of Controlled Release 107, 262–275.
Xiong, X.B., Uludağ, H., Lavasanifar, A., 2010. Virus-mimetic polymeric micelles for targeted siRNA delivery. Biomaterials 31, 5886–5893.
Xiong, X.B., Lavasanifar, A., 2011. Traceable multifunctional micellar nanocarriers for cancer-targeted co-delivery of MDR-1 siRNA and doxorubicin. ACS Nano 5, 5202–5213.
Xu, H., Deng, Y., Chen, D., Hong, W., Lu, Y., Dong, X., 2008. Esterase-catalyzed dePEGylation of pH-sensitive vesicles modified with cleavable PEG-lipid derivatives. Journal of Controlled Release 130, 238–245.
Yang, T., Wang, Y., Li, Z., Dai, W., Yin, J., Liang, L., Ying, X., Zhou, S., Wang, J., Zhang, X., Zhang, Q., 2012. Targeted delivery of a combination therapy consisting of combretastatin A4 and low-dose doxorubicin against tumor neovasculature. Nanomedicine 8, 81–92.